Discovery of Quinolinediones Exhibiting a Heat Shock Response and Angiogenesis Inhibition

Robert H. J. Hargreaves,[†] Cynthia L. David,[‡] Luke J. Whitesell,[§] Daniel V. LaBarbera,[†] Akmal Jamil,[†] Jean C. Chapuis,[†] and Edward B. Skibo*,[†]

Department of Chemistry and Biochemistry, Arizona State University, Tempe, Arizona 85287-1604, Steele Memorial Children's Research Center, University of Arizona, Tucson, Arizona 85724, and Whitehead Institute, Nine Cambridge Center, Cambridge, Massachusetts 02142

Received November 8, 2007

A series of substituted quinoline-5,8-diones were synthesized and evaluated as inhibitors of the chaperone protein Hsp90 using two assays: competition for binding to C-terminal ATP-binding site and competition for binding to N-terminal ATP-binding site. In addition, the ability of the compounds to induce the heat shock response was determined using a reporter fibroblast cell line. Of all the compounds assayed, only 6-aziridinyl-2-biphenylquinoline-5,8-dione induced a heat shock response and did so without interacting at the ATP binding sites of Hsp90. COMPARE analysis was carried out on quinoline-5,8-diones active in the National Cancer Institute's 60-cell line screen with the goal of discovering quinoline-5,8-dione structures that interact with other cellular targets (molecular targets) important for cancer chemotherapy. COMPARE analysis led to the discovery of a combretastatin-like quinoline-5,8-dione structure that, in fact, inhibited angiogenesis.

Introduction

Heat shock protein 90 (Hsp90[a]) is emerging as an important target for cancer chemotherapy because of its role in chaperoning proteins involved in signal transduction pathways that control tumor cell proliferation and survival.[1–3] The prototype inhibitor of Hsp90 is geldanamycin shown in the inset of Chart 1. This complex natural product has been the subject of total synthesis[4,5] and analogue development.[6] In addition, the synthesis and screening of purine libraries has afforded small molecules capable of geldanamycin-like binding to Hsp90.[7–9] This laboratory has approached Hsp90 inhibitor design by molecular modeling and library synthesis.[10] As illustrated in Chart 1, the substituted quinoline quinone ring system has some of the structural elements of geldanamycin. In fact, these studies revealed that some quinoline quinones possess geldanamycin-like cytostatic and cytotoxic activity, based on COMPARE analysis,[11,12] although none actually interact with Hsp90. This report further investigates the ability of diverse quinoline quinones (**1** and **2**) in Chart 1 to interact with Hsp90 and influence protein maturation. One analog of **2** was found to induce the heat shock response consistent with an ability to impair protein homeostasis in cells without directly interacting with the known drug-binding sites on Hsp90.

The quinoline quinone system is also a component in a number of antitumor agents, most notably lavendamycim and streptonigrin shown in Chart 2. Therefore, substituted quinoline quinones could interact with targets important for cancer chemotherapy other than Hsp90. To assess other cellular targets

Chart 1

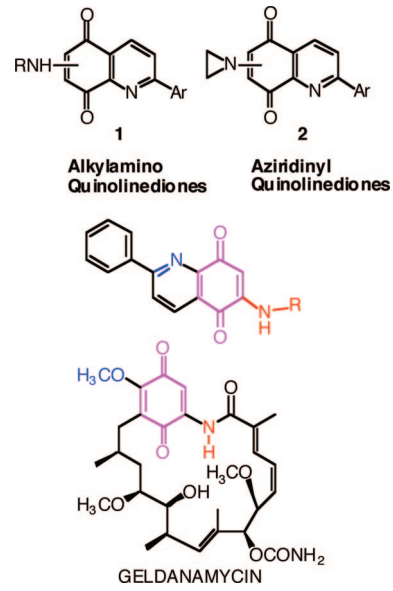

of **1** and **2**, COMPARE analysis [11,12] was carried using National Cancer Institute 60-cell line mean graph data for each compound. Thus, the pattern of cytostatic and cytotoxic parameters, GI_{50} (growth inhibition 50%), TGI (total growth inhibition), and LC_{50} (lethal concentration 50%) on the mean graphs of **1** and **2** was compared with those of over 38000 compounds in the National Cancer Institute's archives. The goals were to find a compound of known mechanism of action and perhaps a molecular target important for cancer chemotherapy. As a result of this screening effort, several new lead compounds directed toward novel molecular targets were discovered. We followed up on one of these leads and document an angiogenesis inhibitor based on the quinoline quinone ring system.

Results and Discussion

Synthesis. The preparation of the target compounds was initiated with the Friedlander quinoline synthesis, Scheme 1.

* To whom correspondence should be addressed. Phone: 480-965-3581. Fax: 480-965-2747. E-mail: eskibo@asu.edu.
† Arizona State University.
‡ University of Arizona.
§ Whitehead Institute.

[a] Abbreviations: Hsp90, heat shock protein; GI_{50}, growth inhibition 50%; TGI, total growth inhibition; LC_{50}, lethal concentration 50%; gHMBC, gradient heteronuclear multiple bond coherence; DMSO, dimethyl sulfoxide; ATP, adenosine triphosphate; EGFP, enhanced green fluorescent protein; mRNA, messenger ribonucleic acid; FGF, fibroblast growth factor; HUVEC, human umbilical vein endothelial cell; NSC, Cancer Chemotherapy National Service Center; FGFRs, fibroblast growth factor receptors; TLC, thin layer chromatography.

10.1021/jm7014099 CCC: $40.75
Published on Web 03/26/2008

Chart 2

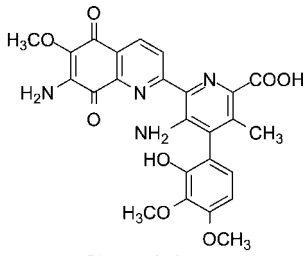

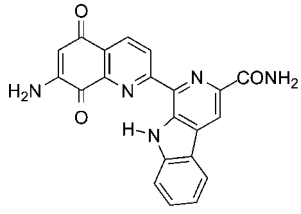

Lavendamycin

Scheme 1

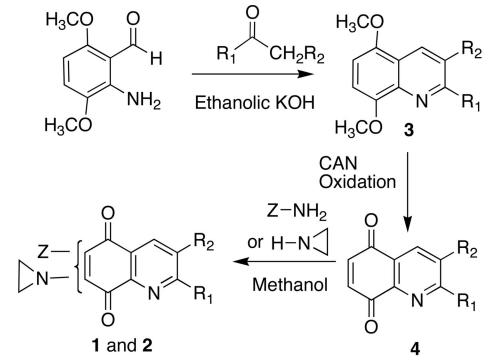

R_1	R_2	**3** and **4**
Phenyl	H	a
Methyl	H	b
3, 4, 5-trimethoxy Phenyl	H	c
Biphenyl	H	d
Methoxy	Methyl	e
Methoxy	Phenyl	f
Methyl	Phenyl	g

Thus, the reaction of 2-amino-3,6-dimethoxybenzaldehyde[13] with the appropriate ketones afforded substituted-5,8-dimethoxyquinolines (**3**). Oxidative demethylation of **3**, to produce substituted quinoline-5,8-diones (**4**), was carried out in high yields with ceric ammonium nitrate, Scheme 1. Treatment of derivatives **4** without a 3-substituent with primary amines or aziridine afforded a mixture of the 6- and 7-amino derivatives **1** and **2**, Tables 1 and 2. In all instances, the isolated yields of the 6-isomer were higher than that of the 7-isomer. We observed that an electron-releasing substituent (methyl and methoxy) at the 3-position directed amination predominately to the 7-position. The 3-substituent releases electrons to the 8-carbonyl, so the Michael-type addition of the amine occurred at the 7-position with negative charge development occurring at the 5-carbonyl. Both the 6- and the 7-isomers of **1** and **2** were evaluated as Hsp90 inhibitors and as cytotoxic and cytostatic agents. Confirmation of the structures of the 6- and 7-isomers was readily carried out using gHMBC (Gradient Heteronuclear Multiple Bond Coherence), as illustrated in Figure 1.

Table 1. Aminoquinolinedione Derivatives

cmpd	2-substituent	6-substituent	7-substituent
1a	phenyl	*N*-pyrrolidino	H
1b	phenyl	benzylamino	H
1c	phenyl	H	benzylamino
1d	phenyl	allylamino	H
1e	phenyl	3-methoxy propylamino	H
1f	phenyl	H	3-methoxy propylamino
1g	3,4,5-trimethoxy phenyl	benzylamino	H
1h	3,4,5-trimethoxy phenyl	H	benzylamino
1i	phenyl	3,4,5-trimethoxy benzylamino	H
1j	phenyl	H	3,4,5-trimethoxy benzylamino
1k	3,4,5-trimethoxy phenyl	methoxy	H

Table 2. Aziridinyl Quinolinedione Derivatives

cmpd	2-substituent	3-substituent	6-substituent	7-substituent
2a	methyl	H	aziridinyl	H
2b	methyl	methoxy	H	aziridinyl
2c	phenyl	methoxy	H	aziridinyl
2d	3,4,5-trimethoxy phenyl	H	aziridinyl	H
2e	biphenyl	H	aziridinyl	H
2f	phenyl	Methyl	aziridinyl	H
2g	phenyl	H	aziridinyl	H
2h	phenyl	H	H	aziridinyl

Hsp90 Inhibition Assays. Assays were carried out on **1** and **2** to assess their ability to interact with previously described drug-binding sites in the C-terminus and N-terminus of Hsp90 and their ability to induce a cellular heat shock response in a manner similar to that of known Hsp90 inhibitors.

Competition for Binding to C-Terminal ATP (Adenosine Triphosphate) Binding Site on Hsp90 Using Immobilized Novobiocin.[14] Compound series **1** and **2** were formulated in DMSO (dimethyl sulfoxide) at 35 mM immediately prior to experiments. Compound solutions were added to whole cell lysates at a final nominal concentration of 100 μM. After drug addition, lysates were incubated on ice for 30 min and then sepharose beads, on which novobiocin had been immobilized, were added followed by incubation at 4 °C with rocking for 60

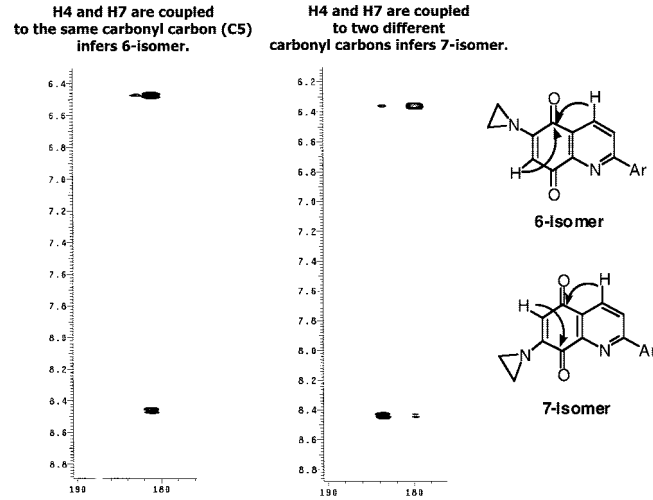

Figure 1. gHMBC spectra of the 6- and 7-isomers of aziridinyl quinolinediones **2g** and **2h**, respectively.

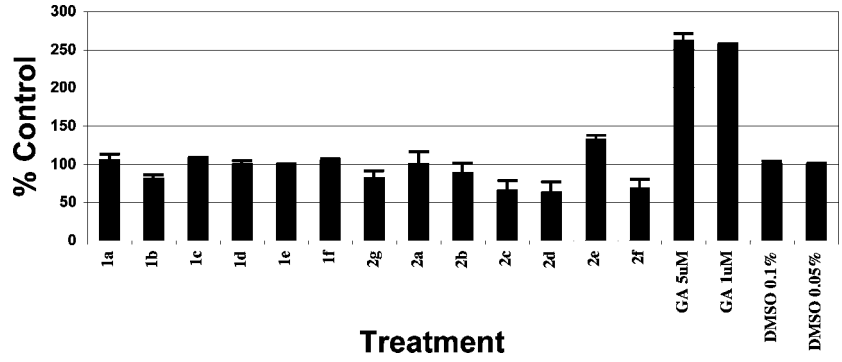

Figure 2. Heat shock response in 3T3Y9/B12 cells. Positive controls consisted of geldanamycin at 1 and 5 μM. Final drug concentrations were 5 μM.

min. The novobiocin beads were then washed, and the proteins were eluted and run on gels, followed by blotting for Hsp90. A positive result consisted of the disappearance of the Hsp90 band, indicating that the drug was able to compete for Hsp90 binding with novobiocin. None of the compounds displayed detectable competition for C-terminal binding of Hsp90. Authentic novobiocin was used at a concentration of 1 mM (partial inhibition of binding) and 10 mM (complete inhibition) as positive controls. It was not possible to test the candidate compounds at these concentrations due to limitation in their aqueous solubility. Thus, it was not possible to compare the candidate compounds to novobiocin directly, but it is safe to say that they demonstrated no inhibitory activity at a concentration far above that which resulted in biological effects in cells.

Competition for Binding to N-Terminal ATP-Binding Site on Hsp90 Using Immobilized Geldanamycin.[15] Candidate compounds were formulated in DMSO immediately prior to experiment at 35 mM. Compound solutions were added to whole cell lysates at a final nominal concentration of 100 μM. This assay was carried out as described above for the C-terminal ATP binding assay, except that geldanamycin was derivatized and immobilized on agarose beads as previously described. A positive result again consisted of disappearance of the Hsp90 band, indicating that the drug was able to compete effectively with the immobilized geldanamycin for Hsp90 binding. None of the compounds displayed N-terminal binding at the ATP binding site of Hsp90 in this assay. Because the candidate compounds were tested at a 6-fold higher concentration than the positive control (geldanamycin), it is safe to conclude that the compounds are at least 6-fold less active than geldanamycin and demonstrated no inhibitory activity at a concentration far above that which resulted in biological effects in cells.

Heat Shock Response in Fibroblasts Stably Transfected with GFP Reporter Construct.[16] Candidate compounds were freshly formulated in DMSO. Compound solutions were added to 3T3Y9/B12 reporter cells that are stably transfected with a heat shock-responsive EGFP (enhanced green fluorescent protein) construct and incubated overnight. Final compound concentrations were 5 μM. Treated wells were evaluated the following day using fluorescence microscopy and a microplate fluorometer. The positive controls consisting of geldanamycin at 1 and 5 μM showed fluorescence exceeding control values (Figure 2). Compound **2e** showed modest activity in this assay although this compound did not bind to Hsp90. This result is most consistent with a secondary or nonspecific effect unrelated to a direct action on the chaperone machinery.

Cytotoxic and Cytostatic Activity, COMPARE Analysis. The mean cytostatic and cytotoxic parameters of **1** and **2** are listed in Tables 3 and 4. The cytostatic parameters include

Table 3. In Vitro Assay Results of Aminoquinolinedione Derivatives

cmpd	mid-range GI_{50} (range)	mid-range TGI and range	mid-range LC_{50} and range
1a	−4.35 (1.77)	inactive	inactive
1b	−5.77 (3.92)	−4.81 (3.08)	−4.18 (1.84)
1c	−4.48 (3.01)	inactive	inactive
1d	−5.72 (3.72)	−4.85 (4.00)	−4.36 (1.77))
1e	−5.45 (2.67)	−4.72 (2.08)	−4.18 (1.38)
1f	−5.26 (2.42)	−4.54 (2.22)	−4.15 (1.58)
1g	inactive	inactive	inactive
1h	−5.57 (2.95)	−4.20 (2.15)	inactive
1i	−5.63 (1.96)	−4.81 (1.99)	−4.18 (1.34)
1j	−4.24 (1.87)	inactive	inactive

Table 4. In Vitro Assay Results of Aziridinylquinolinedione Derivatives

cmpd	mid-range GI_{50} (range)	mid-range TGI and range	mid-range LC_{50} and range
2a	−6.29 (2.14)	−5.69 (1.29)	−5.10 (1.74)
2b	−6.56 (1.47)	−6.08 (1.41)	−5.36 (2.27)
2c	−6.28 (2.30)	−5.78 (1.88)	−5.31 (2.01)
2d	−6.23 (2.15)	−5.75 (1.26)	−5.26 (2.22)
2e	−5.10 (2.61)	−4.57 (2.32)	−4.19 (1.22)
2g	−7.56 (2.07)	−6.49 (2.47)	−5.69 (4.00)
2h	−7.07 (3.21)	−5.48 (4.00)	−4.75 (2.78)

GI_{50} and TGI, which are the concentrations of drug required for 50% growth inhibition and total growth inhibition, respectively. The cytotoxic parameter is the LC_{50}, which is the concentration required for 50% cell kill. These in vitro data were obtained under the In Vitro Cell Line Screening Project at the National Cancer Institute.[11,17–20] The log mean values for GI_{50}, TGI, and LC_{50} in 60 cell lines are provided in Tables 3 and 4 along with the log range (the maximum difference between the least-sensitive and the most-sensitive cell lines). The log range parameter has been used to gain insights into the selectivity of antitumor agents.[21] The "inactive" category pertains to compounds with log mean values of −4 with log range values of 0 to 1.

COMPARE analysis[11,12] provided insights into what might be the molecular target of the active analogues of **1** and **2** exhibiting high selectivity (compounds with bold borders in Tables 3 and 4). The criteria for choosing active compounds for COMPARE analysis include: log mean values <-4 with log range values of >2, and with high selectivity for 10 or more cell lines and/or selectivity for specific histologies. The mean graphs of compounds meeting these criteria have distinctive patterns amenable to meaningful COMPARE analysis. In contrast, mean graphs with low log range values are essentially flat and will correlate with other such mean graphs without meaningful target information.

Chart 3

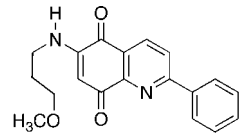

1e

Molecular target=
Fibroblast Growth Factor
(FGF-2)
cc = 0.56

Compares with

cc = 0.7

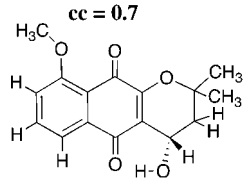

5

Chart 4

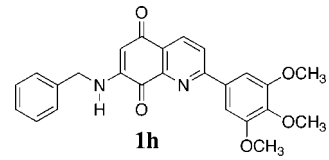

1h

Molecular Target
Erythrocyte binding protein,
cc = 0.6

Compares with

cc = 0.77

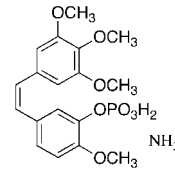

6

The pattern of cytostatic and cytotoxic parameters (GI_{50}, TGI, and LC_{50} mean graphs) of selected analogues of **1** and **2** were compared with those of over 38000 compounds in the National Cancer Institute's archives. The goal was to find a compound of known mechanism of action and perhaps a molecular target that correlated well with the mean graphs of the selective analogues of **1** and **2**. Thus, these analogues were used as a seed compound in the following NCI databases: Standard Agent database, Synthetic Agent database, and the Molecular Targets Database. The Standard Agent Database consists of 175 drugs with cancer treatment applications as well as new compounds with a high level of interest.[17] Molecular target levels (e.g., topoisomerase II, DT-diaphorase, proteins of unknown function, etc.) have been measured in the 60-cell line panel using mRNA (messenger ribonucleic acid) expression and enzyme activity levels.[22]

The results of COMPARE analysis are discussed below for compounds **1e**, **1h**, and **2g**,**h**. The rest of the active compounds did not exhibit significant correlations with known molecular targets. It is noteworthy that COMPARE analysis reveled that none of the aziridinyl quinone derivatives were dependent on DT-diaphorase for activity. This two-electron reducing enzyme typically activates aziridinyl quinones as cytotoxic alkylating agents.

Compound **1e**, and to a lesser degree the isomer **1f**, correlated well with the naphthoquinone natural product **5** (NSC 679186;[23] NSC, Cancer Chemotherapy National Service Center) as well as with fibroblast growth factor (FGF-2), Chart 3. The natural product has been reported to be cytotoxic and had a moderate correlation with the dual specificity protein phosphatase CDC 25A.[24] There are obvious structural similarities between **1e** and **5**, particularly the oxygen-containing side chain of both compounds. The FGF-2 molecular target plays an important role in cell growth and has been the target of antitumor agent design.[25–27] The fibroblast growth factors interact with the receptor tyrosine kinases (FGFRs) in conjunction with heparin-binding coreceptors. Indeed, reported FGF-2 inhibitors are heterocycles tethered to glucuronide derivatives.[25] Perhaps the oxygenated side chain of **1e** plays a role in the FGF-2 inhibition through mimicry of a carbohydrate residue.

Compound **1h** correlated well with both the antimitotic agent combretastatin A-4,[28] compound **6** (NSC 64001) in Chart 4, and the molecular target erythrocyte binding protein. The correlation coefficient of 0.8 was the highest we observed in our COMPARE analyses. Significantly, this molecular target is involved in mitosis[29] and, therefore, **1h** is mechanistically similar to **6**. In addition, the structures of both compounds are nearly superimposable, except for the benzylamino group of **1h**. This additional substituent was considered responsible for the lower potency of **1h** compared to **6**. In the following section, we provide evidence that validates these findings.

Compounds **2g**,**h** are the only active aziridinyl derivatives that correlate with well-characterized molecular targets, the protein tyrosine phosphatases.[10] In contrast, compound **2c** exhibits high correlations with MAP7 gene-expressed proteins.[22] The high specificity of **2c** for leukemia and renal cancers, as well as the possibility of exploiting a new molecular target, make this analogue worthy of further investigation.

Antiangiogenesis Assays. We were intrigued by the high correlation of compound **1h** with both the antimitotic agent **6** and erythrocyte binding protein. To validate this result, we assayed **1h**, **1g**, and **1k** in the HUVEC inhibition and angiogenesis assays. Compound **6** exerts its antitumor activity by inhibiting angiogenesis, the development of new blood vessels that permits tumor growth. Compounds **1h** and **1g** were assayed to determine the possible role of the benzylamino group in inhibiting angiogenesis. A model obtained by superimposing **6** onto the quinolinedione nucleus suggested that the 6-methoxy derivative **1k** would be a better combretastatin mimic than **1h** and **1g**, Figure 3.

The HUVEC assay utilizes human umbilical vein endothelial cells to evaluate the inhibition of cell growth as well as the inhibition of cord and junction formation on a basement membrane matrix. The control picture in Figure 4 shows untreated cells forming cords and junctions in the matrix. Both **1h** and **1g** show a significant decrease in cord length and junction formation at 10 μg/mL along with 23% growth inhibition. Parallel inhibition assays[LW1] against HUVEC, NCI-H460 (nonsmall-cell lung cancer), and MCF-7 (breast cancer) revealed that both **1h** and **1g** inhibited the proliferation of cancer cells more than the endothelial cells. These results indicate that **1h** and **1g** possess some antiangiogenesis activity, but that another mechanism may be responsible for the stronger cancer cell inhibition. In contrast, compound **1k** showed complete inhibition of cord and junction formation at 10 μg/mL[LW2]. Furthermore, both the endothelial cells and the MCF-7 cancer cells are equally sensitive to **1k**. In fact, the

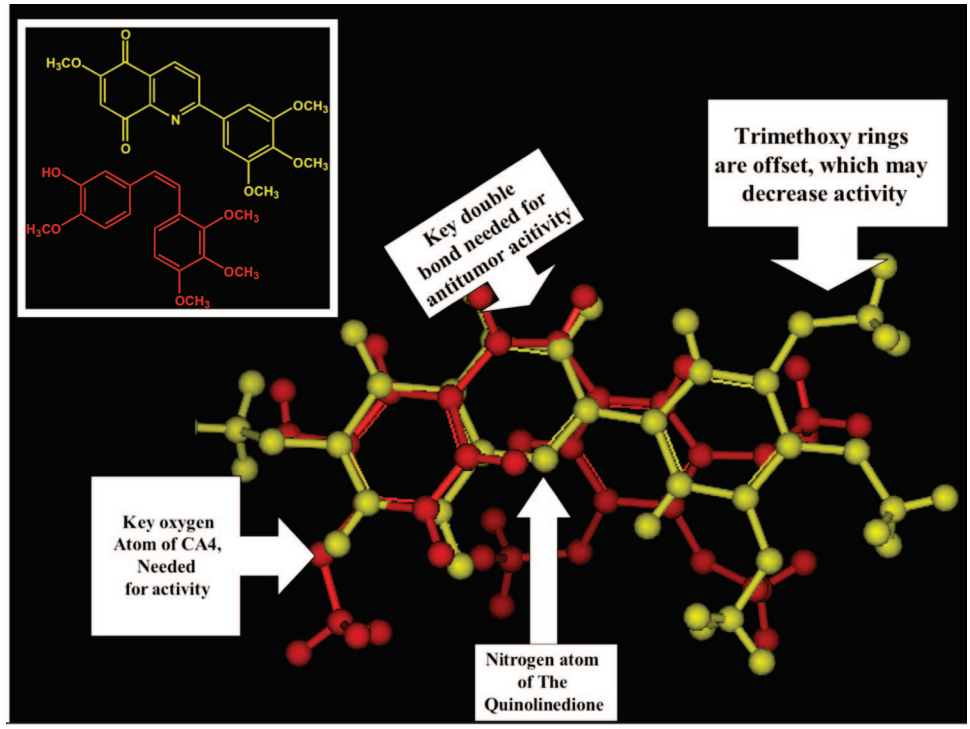

Figure 3. Superimposed minimized structures of the combretastatin **6** (red) and the quinolinedione **1k** (yellow).

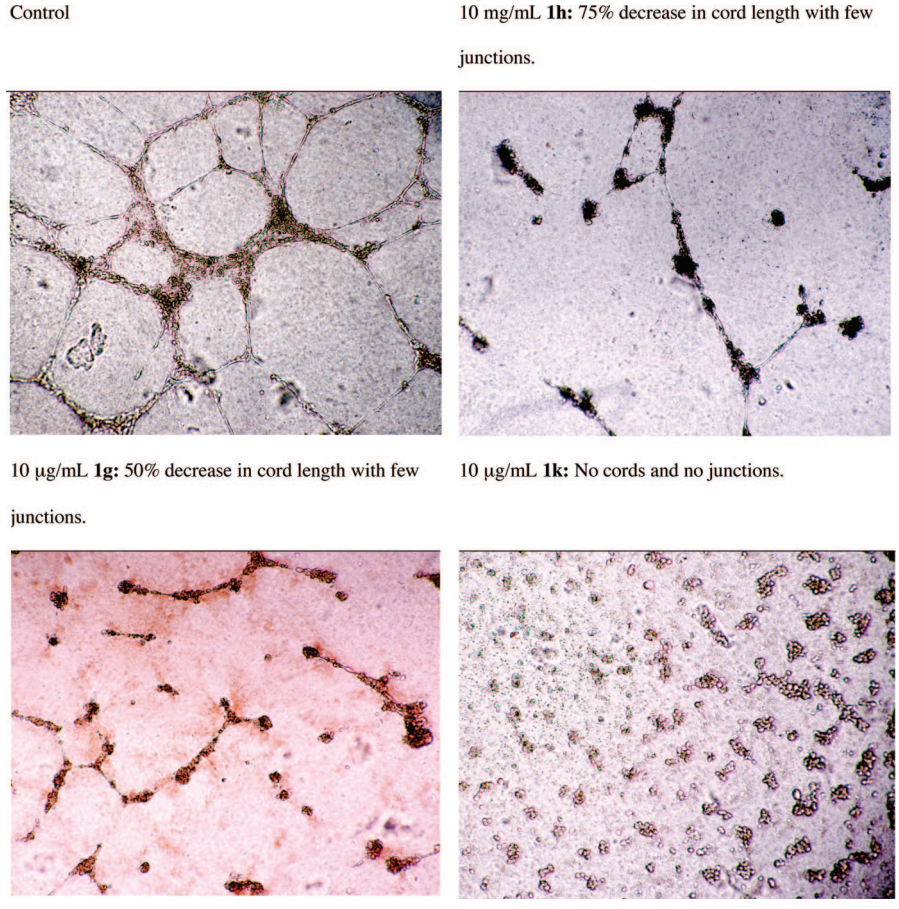

Figure 4. Endothelial cells in the HUVEC angiogenesis assay either untreated or treated with 10 μg/mL of **1h**, **1g**, or **1k**.

combretastatin A-4-treated endothelial cells are identical in appearance to those treated with **1k**. However, compound **6** is about a 1000-fold more potent than **1k**. We believe that the altered position of the trimethoxyphenyl group of **1k** is the main reason for the decreased potency, see Figure 3. Although compound **1k** is not as potent as compound **6**, it may still prove to be a useful antitumor agent if it possesses low toxicity and suitable solubility. Lastly, the mechanism of antiangiogenesis

exhibited by **1k** is unknown at this time and a future publication will address this point.

Conclusions

The Hsp90 screening and the COMPARE analysis of the quinolinedione libraries **1** and **2** resulted in four leads.

Compound **2e** modestly induced the heat shock response in fibroblasts although it does not compete with ATP for binding at either the C-terminal or N-terminal sites of Hsp90. The biological significance of this result is as yet unknown.

Compound **1e** mean graph data correlated well with the fibroblast growth factor (FGF-2) molecular target and there are some structural similarities with reported FGF-2 inhibitors. It may be possible to design other such inhibitors by tethering oxygenated side chains to heterocyclic quinones.

Compound **1h** is considered to be an analogue of compound **6** based on COMPARE analysis and structural similarities. We verified that analogues **1h**, **1g**, and **1k** are inhibitors of angiogenesis. Similarly, combretastatin A-4 exerts its antitumor activity by inhibiting angiogenesis.

Compounds **2g**,**h** are the only active aziridinyl derivatives that correlated with well-characterized molecular targets, the protein tyrosine phosphatases.[10] Ongoing analogue development, where the aziridinyl group of **2g**,**h** is substituted for other alkylating moieties, has yet to yield equally active compounds.

Compound **2c** displayed some histological selectivity (leukemia and renal) without correlating with a known cancer chemotherapeutic molecular target. This finding suggests that **2c** may be a novel antitumor agent directed toward an as-yet-uncharacterized molecular target and, therefore, should be the focus of further analogue development.

Finally, this study illustrates the value of COMPARE analysis in mining a library of compounds for novel structures that correlate with molecular targets useful for cancer chemotherapy. The present study provides criteria for selecting compounds for COMPARE analysis. The goal of the present effort was to discover other molecular targets for the quinolinediones besides the intended target, Hsp90. In future studies, the quinolinediones selected from the COMPARE analysis (**2e**, **1e**, **1h**, **2g**, **2h**, and **2c**) will be lead compounds for novel drug development. A recent example of this means of drug discovery was the discovery of a novel IMP dehydrogenase inhibitor structure among a series of DNA cleaving agents.[30] Molecular modeling and analogue development has validated this COMPARE result.

Experimental Section

All analytically pure compounds were dried under high vacuum in a drying pistol over refluxing methanol. Many of the compounds crystallized from reaction mixtures or elution solvents upon concentration and therefore no recrystallization solvent is specified. Elemental analyses of final products that were assayed were run at Atlantic Microlab, Inc., Norcross, Ga. Melting points and decomposition points were determined with a Mel-Temp apparatus. All TLCs were performed on silica gel plates using a variety of solvent systems and a fluorescent indicator for visualization. IR spectra were taken as KBr pellets and only the strongest absorbances were reported. ^{1}H NMR spectra were obtained with a 300 or 500 MHz spectrometer. All chemical shifts are reported relative to TMS.

The following heat shock protein-related assays were carried out as previously described: Competition for binding to C-terminal ATP-binding site on Hsp90 using immobilized novobiocin,[14] competition for binding to N-terminal ATP-binding site on Hsp90 using immobilized geldanamycin,[15] and heat shock response in fibroblasts stably transfected with GFP reporter construct.[16] All stock solutions of **1** and **2** were prepared fresh in DMSO.

Analogues of **1** and **2** shown in Tables 3 and 4 were screened in the National Cancer Institute's 60-cell line screen.[11,17–20] Mean graph results were then analyzed with COMPARE.[11,12]

2-(3,4,5-Trimethoxyphenyl)-5,8-dimethoxyquinoline (3c). A solution of 2-amino-3,6-dimethoxybenzaldehyde (0.65 g, 3.59 mmol), 3,4,5-trimethoxyacetophenone (0.83 g, 3.95 mmol), and 10% ethanolic KOH (2 mL) was refluxed under nitrogen for 21 h. The reaction mixture was cooled and the solvent removed in vacuo to yield a yellow oil, which was purified by flash chromatography (SiO_2, ethyl acetate/hexanes (1:1)) to yield colorless crystals: 0.84 g (66% yield); mp 110.5–111.5 °C; TLC (ethyl acetate/hexanes [1:1]) $R_f = 0.27$; ^{1}H NMR (300 MHz, $CDCl_3$) δ 8.59 (d, $J = 9$ Hz, 1H), 7.85 (d, $J = 9$ Hz, 1H), 7.40 (s, 2H), 6.96 (d, $J = 8.7$ Hz, 1H), 6.75 (d, $J = 8.7$ Hz, 1H), 4.06 (s, 3H), 4.00 (s, 6H), 3.98 (s, 3H), 3.91 (s, 3H); ^{13}C NMR (100 MHz, $CDCl_3$) δ 156.27, 153.44, 149.45, 148.67, 140.30, 139.37, 135.46, 131.65, 120.32, 118.40, 107.70, 104.99, 103.48, 60.88, 56.24, 56.17, 55.69; MS 355 (M^+), 340, 326, 310, 282, 252, 196, 177.

2-(4-Biphenyl)-5,8-dimethoxyquinoline(3d). A solution of 2-amino-3,6-dimethoxybenzaldehyde (0.75 g, 4.14 mmol), 4-acetylbiphenyl (0.9 g, 4.58 mmol) and 10% ethanolic KOH (2 mL) in ethanol (50 mL) was refluxed under nitrogen for 20 h. The solution was cooled in an ice/water bath and the crystals filtered, washed with ice cold ethanol, and dried: 1.20 g (85% yield); mp 162–162.5 °C; TLC (ethyl acetate/hexanes [1:1]) $R_f = 0.69$; ^{1}H NMR (500 MHz, $CDCl_3$) δ 8.61 (d, $J = 8.5$ Hz, 1H), 8.29 (d, $J = 8$ Hz, 2H), 7.94 (d, $J = 8.5$ Hz, 1H), 7.74 (d, $J = 8$ Hz, 2H), 7.67 (d, $J = 7$ Hz, 2H), 7.46 (t, $J = 7.5$, 2H), 7.37 (t, $J = 7.5$ Hz, 1H), 6.96 (d, $J = 9$ Hz, 1H), 6.74 (d, $J = 9$ Hz, 1H), 4.07 (s, 3H), 3.97 (s, 3H); ^{13}C NMR (125 MHz, $CDCl_3$) δ 156.06, 149.67, 148.78, 141.89, 140.64, 140.59, 138.50, 131.68, 128.78, 128.04, 127.48, 127.10, 120.48, 118.34, 107.72, 103.52, 56.40, 55.76; MS 341 (M^+), 326, 312, 297, 283, 268, 254, 178.

3,5,8-Trimethoxy-2-methylquinoline(3e). A solution of 2-amino-3,6-dimethoxybenzaldehyde (1 g, 5.52 mmol), methoxyacetone (1 g, 1.04 mL, 11.4 mmol), and ethanolic KOH (10%, 2 mL) in ethanol (50 mL) was refluxed under nitrogen for 30 min. The reaction mixture was cooled and the solvent removed in vacuo. The resulting oil was purified by flash column chromatography (SiO_2, chloroform/methanol [98:2]) to yield a white solid (1.14 g, 89%); mp 117–8 °C; TLC (ethyl acetate/hexanes [1:1]) $R_f = 0.28$; ^{1}H NMR (300 MHz, $CDCl_3$) δ 7.67 (s, 1H), 6.77 (d, $J = 8.5$ Hz, 1H), 6.71 (d, $J = 8.5$ Hz, 1H), 4.02 (s, 3H), 3.97 (s, 3H), 3.96 (s, 3H), 2.69 (s, 3H); ^{13}C NMR (100 MHz, $CDCl_3$) δ 152.12, 151.83, 148.93, 147.63, 134.20, 121.45, 106.61, 103.82, 103.45, 55.90, 55.66, 55.30, 20.75; MS 233 (M^+), 218, 204, 175, 160, 83.

3,5,8-Trimethoxy-2-phenylquinoline (3f). A solution of 2-amino-3,6-dimethoxybenzaldehyde (1 g, 5.52 mmol), 2-methoxyacetophenone (0.83 g, 5.53 mmol), and ethanolic KOH (10%, 2 mL) in ethanol (50 mL) was refluxed under nitrogen for 1 h. The reaction mixture was cooled, and the solvent was removed in vacuo. The resulting oil was purified using flash column chromatography (SiO_2, dichloromethane) to yield a white solid (1.17 g, 72%); mp 124–5 °C; TLC (ethyl acetate/hexanes [1:1]) $R_f = 0.61$; ^{1}H NMR (300 MHz, $CDCl_3$) δ 8.02 (m, 2H), 7.84 (s, 1H), 7.43 (m, 3H), 6.77 (d, $J = 8.4$ Hz, 1H), 6.70 (d, $J = 8.4$ Hz, 1H), 3.99 (s, 3H), 3.94 (s, 6H); ^{13}C NMR (75 MHz, $CDCl_3$) δ 151.71, 150.39, 149.74, 147.60, 137.86, 134.99, 129.94, 128.52, 127.77, 121.84, 108.32, 104.57, 104.11, 56.06, 55.62, 55.41; MS 295 (M^+), 280, 266, 250, 236.

5,8-Dimethoxy-3-methyl-2-phenylquinoline (3g). A solution of 2-amino-3,6-dimethoxybenzaldehyde (1 g, 5.52 mmol), propiophenone (0.73 mL, 0.75 g, 5.60 mmol), and 10% ethanolic KOH (2 mL) was refluxed under nitrogen for 19 h. The solution was cooled and the solvent removed in vacuo to yield an oil, which was purified by flash chromatography (SiO_2, ethyl acetate/hexanes [1:1]) to afford a white solid; 1.06 g (69% yield); mp 145.5–146.5 °C; TLC (ethyl acetate/hexanes [1:1]) $R_f = 0.59$; ^{1}H NMR (300 MHz, $CDCl_3$) δ 8.39 (s, 1H), 7.62 (m, 2H), 7.42 (m, 3H), 6.87 (d, $J = 8.2$ Hz, 1H), 6.72 (d, $J = 8.2$ Hz, 1H), 4.00 (s, 3H), 3.96 (s, 3H), 2.47 (s, 3H); ^{13}C NMR (125 MHz, $CDCl_3$) δ 159.50, 149.67, 148.14,

141.02, 138.98, 131.65, 129.27, 128.96, 128.02, 127.97, 120.85, 106.20, 103.53, 56.08, 55.75, 20.74; MS 279 (M^+), 264, 250, 235, 220, 191.

2-(3,4,5-Trimethoxy)quinoline-5,8-dione (4c). To a solution of **3c** (350 mg, 0.99 mmol) in acetonitrile (30 mL) was added dropwise a solution of ceric ammonium nitrate (1.35 g, 2.46 mmol) in water (30 mL). After one hour, the resulting precipitate was filtered, washed with water, and dried to yield a dark red solid: 177 mg (55% yield); mp 166–7 °C; TLC (ethyl acetate/hexanes [1:1]) R_f = 0.17; ^{1}H NMR (300 MHz, $CDCl_3$) δ 8.45 (d, J = 8.2 Hz, 1H), 8.06 (d, J = 8.2 Hz, 1H), 7.41 (s, 1H), 7.16 (d, J = 10.5 Hz, 1H), 7.07 (d, J = 10.5 Hz, 1H), 4.00 (s, 6H), 3.93 (s, 3H); MS 325 (M^+), 310, 282, 252, 196, 140.

2-(4-Biphenyl)-quinoline-5,8-dione (4d). To a solution of **3d** (0.55 g, 1.61 mmol) in acetonitrile (25 mL) was added dropwise a solution of ceric ammonium nitrate (2 g, 3.65 mmol) in water (25 mL). After 40 min., the resulting yellow precipitate was filtered, washed with water and dried: 425 mg (85% yield); mp 221–222 °C; TLC (ethyl acetate/hexanes [1:1]) R_f = 0.45; H NMR (500 MHz, $CDCl_3$) δ 8.46 (d, J = 8 Hz, 1H), 8.27 (d, J = 8.5 Hz, 2H), 8.15 (d, J = 8 Hz, 1H), 7.76 (d, J = 8.5 Hz, 2H), 7.67 (d, J = 7.5 Hz, 2H), 7.48 (t, J = 7.5 Hz, 2H), 7.40 (t, J = 7.5 Hz, 1H), 7.16 (d, J = 10.5 Hz, 1H), 7.06 (d, J = 10.5 Hz, 1H); ^{13}C NMR (125 MHz, $CDCl_3$) δ 184.48, 183.30, 161.60, 147.39, 143.55, 140.03, 139.07, 137.94, 136.06, 135.36, 128.90, 128.22, 127.93, 127.67, 127.47, 127.13, 123.89; MS 311 (M^+), 283, 254, 228, 178, 84.

3-Methoxy-2-methylquinoline-5,8-dione (4e). To a stirred solution **3e** (0.5 g, 2.15 mmol) in acetonitrile (25 mL) was added dropwise a solution of ceric ammonium nitrate (2.93 g, 5.35 mmol) in water (25 mL). After 1 h, the reaction mixture was extracted with dichloromethane (3×75 mL), the organic layers were combined and dried (Na_2SO_4), and the solvent was removed in vacuo to yield a yellow solid. This was crystallized from chloroform/hexanes to yield yellow crystals: 355 mg (81% yield); mp 156–7 °C dec; TLC (ethyl acetate/hexanes [1:1]) R_f = 0.19; ^{1}H NMR (300 MHz, $CDCl_3$) δ 7.62 (s, 1H), 7.05 (d, J = 10.5 Hz, 1H), 6.97 (d, J = 10.5 Hz, 1H), 4.02 (s, 3H), 2.66 (s, 3H); MS 203 (M^+), 203, 188, 175, 160, 132.

3-Methoxy-2-phenylquinolin-5,8-dione (4f). To a stirred solution of **3f** (0.5 g, 1.69 mmol) in acetonitrile (30 mL) was added dropwise a solution of ceric ammonium nitrate (2.32 g, 4.23 mmol) in water (30 mL). After one hour, the resulting precipitate was filtered, washed with water, and dried to afford an orange solid: 410 mg (91% yield); mp 197–8 °C dec; TLC (ethyl acetate/hexanes [1:1]) R_f = 0.35; ^{1}H NMR (300 MHz, $CDCl_3$) δ 8.01 (m, 2H), 7.81 (s, 1H), 7.46 (m, 3H), 7.09 (d, J = 10.5 Hz, 1H), 7.01 (d, J = 10.5 Hz, 1H), 4.04 (s, 3H); ^{13}C NMR (75 MHz, $CDCl_3$) δ 185.08, 182.39, 156.73, 153.47, 139.29, 137.37, 135.84, 129.94, 129.79, 129.29, 128.10, 113.86, 56.34; MS 265 (M^+), 264, 250, 236, 207, 140.

3-Methyl-2-phenylquinolin-5,8-dione (4g). To a stirred solution of **3g** (0.5 g, 1.79 mmol) in acetonitrile (30 mL) was added dropwise a solution of ceric ammonium nitrate (2.45 g, 4.47 mmol) in water (20 mL). After 30 min, water (50 mL) was added and the solution stirred for a further 5 min. The mixture was then filtered, and the pale yellow solid was washed well with water and dried: 373 mg (84% yield); mp > 210 °C dec; TLC (ethyl acetate/hexanes [1:1]) R_f = 0.32; ^{1}H NMR (300 MHz, $CDCl_3$) δ 8.28 (s, 1H), 7.58 (m, 2H), 7.48 (m, 3H), 7.13 (d, J = 10.5 Hz, 1H), 7.04 (d, J = 10.5 Hz, 1H), 2.53 (s, 3H); MS 248 (M^+ − H) 220, 191, 166, 139, 115.

2-Phenyl-6-pyrrolidinylquinoline-5,8-dione (1a). To a stirred solution of **4a** (200 mg, 0.85 mmol) in ethanol (15 mL) was added pyrrolidine (142 μL, 121 mg, 1.7 mmol). After 4 h, the reaction mixture was filtered and the red solid was washed with ice-cold ethanol and dried. This solid was crystallized from chloroform/hexanes to afford **1a** as red crystals: 187 mg (72% yield); mp 182–183 °C dec; TLC (chloroform/methanol [49:1]) R_f = 0.40; ^{1}H NMR (400 MHz, $CDCl_3$) δ 8.36 (d, J = 8.4 Hz, 1H), 8.20 (m, 2H), 7.96 (d, J = 8.4 Hz, 1H), 7.49 (m, 3H), 5.95 (s, 1H), 3.99 (bs, 2H), 3.38 (bs, 2H), 2.01 (m, 4H); ^{13}C NMR (100 MHz, $CDCl_3$) δ 182.50, 180.64, 161.71, 148.79, 148.25, 137.73, 135.23, 130.34, 128.77, 127.78, 126.71, 122.18, 106.08, 50.88, 26.59, 23.78; HRMS (EI) m/z, 304.1207; requires, 304.1212.

6-Benzylamino-2-phenylquinoline-5,8-dione (1b) and 7-Benzylamino-2-phenylquinoline-5,8-dione (1c). To a stirred solution of **4a** (200 mg, 0.85 mmol) in ethanol (15 mL) was added benzylamine (186 mL, 182 mg, 1.7 mmol). After 4 h, the reaction mixture was filtered and the red solid was washed with ice-cold ethanol and dried. This solid was purified by flash chromatography (SiO_2, ethyl acetate/hexanes [2:3]) to give **1b** and **1c**.

Compound **1b** was recrystallized from chloroform/hexanes as orange crystals: 46 mg (16% yield); mp 208–209 °C; TLC (chloroform/methanol [49:1]) R_f = 0.76; ^{1}H NMR (500 MHz, $CDCl_3$) δ 8.46 (d, J = 8.5 Hz, 1H), 8.14 (m, 2H), 8.07 (d, J = 8.5 Hz, 1H), 7.32–7.54 (m, 8H), 6.41 (t, J = 5.5 Hz, 1H), 5.85 (s, 1H), 4.43 (d, J = 5.5 Hz, 2H); ^{13}C NMR (125 MHz, $CDCl_3$) δ 182.12, 180.41, 160.83, 148.36, 146.82, 137.88, 135.83, 135.39, 130.56, 129.34, 129.32, 129.21, 128.46, 127.84, 127.81, 125.02, 101.50, 47.20. Anal. ($C_{22}H_{16}N_2O_2 \cdot 0.3H_2O$) C, H, N.

Compound **1c** was recrystallized from chloroform/hexanes as red crystals: 80 mg (28% yield); mp 168–170 °C; TLC (chloroform/methanol [49:1]) R_f = 0.67; ^{1}H NMR (500 MHz, $CDCl_3$) δ 8.41 (d, J = 8.5 Hz, 1H), 8.19 (m, 2H), 7.99 (d, J = 8.5 Hz, 1H), 7.31–7.53 (m, 8H), 6.21 (t, J = 5.5 Hz, 1H), 6.00 (s, 1H), 4.41 (d, J = 5.5 Hz, 2H); ^{13}C NMR (125 MHz, $CDCl_3$) δ 181.42, 181.36, 162.41, 149.22, 147.28, 137.61, 135.57, 135.05, 130.63, 129.06, 128.91, 128.24, 127.86, 127.67, 125.73, 122.49, 102.88, 46.87. Anal. ($C_{22}H_{16}N_2O_2$) C, H, N.

6-Allylamino-2-phenylquinoline-5,8-dione (1d). To a stirred solution of **4a** (200 mg, 0.85 mmol) in ethanol (15 mL) was added allylamine (191 μL, 145 mg, 2.55 mmol). After 2 h, the reaction mixture was filtered and the red solid was washed with ice-cold ethanol and dried. This solid was purified by flash chromatography (SiO_2, ethyl acetate/hexanes [2:3]) to give **1d** as the major isomer that was recrystallized from dichloromethane/hexanes as a red solid: 61 mg (25% yield); mp 187–188 °C dec; TLC (chloroform/methanol [49:1]) R_f = 0.37; ^{1}H NMR (300 MHz, $CDCl_3$) δ 8.41 (d, J = 8.1 Hz, 1H), 8.19 (m, 2H), 8.00 (d, J = 8.1 Hz, 1H), 7.52 (m, 3H), 6.02 (m, 1H), 5.97 (s, 1H), 5.89 (m, 1H), 5.29–5.38 (m, 2H), 3.88 (m, 2H); ^{13}C NMR (125 MHz, $CDCl_3$) 181.40, 181.34, 162.38, 149.21, 147.32, 137.60, 135.04, 131.33, 130.62, 128.90, 127.84, 125.71, 122.46, 118.48, 104.73, 102.70, 44.94. Anal. ($C_{18}H_{14}N_2O_2 \cdot 0.2H_2O$) C, H, N.

6-(3-Methoxypropylamino)-2-phenylquinoline-5,8-dione (1e) and 7-(3-Methoxypropylamino)-2-phenylquinoline-5,8-dione (1f). To a stirred solution of **4a** (200 mg, 0.85 mmol) in ethanol (15 mL) was added 3-methoxypropylamine (174 μL, 1.71 mmol). After 2 h, the solvent was removed in vacuo, and the residue was purified by flash chromatography (SiO_2, ethyl acetate/hexanes [1:1]) to give **1e** and **1f** as products.

Compound **1e** was recrystallized from dichloromethane/hexanes as a red solid: 102 mg (37% yield); mp 165–166 °C; TLC (chloroform/methanol [49:1]) R_f = 0.37; ^{1}H NMR (300 MHz, $CDCl_3$) δ 8.39 (d, J = 8.1 Hz, 1H), 8.20 (m, 2H), 7.98 (d, J = 8.1 Hz, 1H), 7.50 (m, 3H), 6.49 (m, 1H), 5.95 (s, 1H), 3.55 (t, J = 5.4 Hz, 2H), 3.40 (s, 3H), 3.34 (q, J = 6 Hz, 2H), 1.98 (quint, J = 6 Hz, 2H). Anal. ($C_{19}H_{18}N_2O_3$) C, H, N.

Compound **1f** was recrystallized from dichloromethane/hexanes as a red solid: 11 mg (4% yield); ^{1}H NMR (300 MHz, $CDCl_3$) 8.47 (d, J = 8.1 Hz, 1H), 8.14 (m, 2H), 8.06 (d, J = 8.1 Hz, 1H), 7.49 (m, 3H), 6.66 (m, 1H), 5.79 (s, 1H), 3.55 (t, J = 6 Hz, 2H), 3.40 (s, 3H), 3.35 (q, J = 6 Hz, 2H), 1.99 (pent, J = 6 Hz, 2H). The low yield precluded elemental analysis; spectroscopic analysis was consistent with the structure **1f**.

6-Benzylamino-2-(3,4,5-trimethoxyphenyl)-quinoline-5,8-dione (1g) and 7-Benzylamino-2-(3,4,5-trimethoxyphenyl)-quinoline-5,8-dione (1 h). To a stirred solution of **4c** (200 mg, 0.62 mmol) in ethanol (15 mL) was added benzylamine (134 μL, 1.23 mmol). After 2 h, the reaction mixture was filtered and the red solid was washed with ice-cold ethanol and dried. This solid was purified by flash chromatography (SiO_2, ethyl acetate/hexane [1:1]) to afford **1g** and **1h**.

Compound **1g** was crystallized from chloroform/hexanes to afford an orange crystalline product: 119 mg (45% yield); mp 221–222 °C dec; TLC (chloroform/methanol [49:1]) $R_f = 0.51$; ^{1}H NMR (500 MHz, $CDCl_3$) 8.38 (d, $J = 8$ Hz, 1H), 7.93 (d, $J = 8$ Hz, 1H), 7.41 (s, 2H), 7.40–7.30 (m, 5H), 6.22 (t, $J = 5$ Hz, 1H), 5.99 (s, 1H), 4.41 (d, $J = 5$ Hz, 2H), 3.99 (s, 6H), 3.92 (s, 3H); ^{13}C NMR (125 MHz, $CDCl_3$) 181.31, 181.26, 162.01, 153.58, 149.09, 147.31, 140.66, 135.56, 134.98, 133.23, 129.06, 128.26, 127.72, 125.53, 122.29, 105.26, 102.79, 60.97, 56.38, 46.89. Anal. ($C_{25}H_{22}N_2O_5 \cdot 0.3H_2O$) C, H, N.

Compound **1h** was crystallized from chloroform/hexanes to afford an orange crystalline product: 46 mg (17% yield); mp 203–204 °C; TLC (chloroform/methanol [49:1]) $R_f = 0.64$; ^{1}H NMR (500 MHz, $CDCl_3$) 8.45 (d, $J = 8.1$ Hz, 1H), 8.01 (d, $J = 8.1$ Hz, 1H), 7.39–7.31 (m, 7H), 6.37 (t, $J = 6$ Hz, 1H), 5.85 (s, 1H), 4.44 (d, $J = 6$ Hz, 2H), 3.99 (s, 6H), 3.92 (s, 3H); ^{13}C NMR (125 MHz, $CDCl_3$) δ 182.05, 180.30, 160.44, 153.89, 146.29, 146.65, 140.55, 135.79, 135.32, 133.43, 129.30, 129.16, 128.46, 127.79, 124.79, 123.00, 105.15, 101.47, 61.20, 56.56, 47.16. Anal. ($C_{25}H_{22}N_2O_5 \cdot 0.3H_2O$) C, H, N.

2-Phenyl-6-(3,4,5-trimethoxybenzylamino)quinoline-5,8-one (1i) and 2-Phenyl-7-(3,4,5-trimethoxybenzylamino)quinoline-5,8-one (1j). To a stirred solution of **4a** (380 mg, 1.62 mmol) in ethanol (25 mL) was added 3,4,5-trimethoxybenzylamine (0.55 mL, 3.2 mmol). After 4 h, the reaction mixture was filtered and the orange solid washed with ice-cold ethanol and dried. This solid was purified by flash chromatography (SiO_2, ethyl acetate/hexanes [1:1]) to give **1i** and **1j**.

Compound **1i** was crystallized from chloroform/hexanes as a dark orange crystals: 264 mg (38% yield); mp 198–199 °C dec; TLC (chloroform/methanol [49:1]) $R_f = 0.56$; ^{1}H NMR (500 MHz, $CDCl_3$) δ 8.42 (d, $J = 8.4$ Hz, 1H), 8.19 (m, 2H), 8.01 (d, $J = 8.4$ Hz, 1H), 7.51 (m, 3H), 6.54 (s, 2H), 6.16 (t, $J = 5.4$ Hz, 1H), 6.02 (s, 1H), 4.34 (d, $J = 5.4$ Hz, 2H), 3.87 (s, 6H), 3.86 (s, 3H); ^{13}C NMR (125 MHz, $CDCl_3$) 181.45, 181.35, 162.47, 153.74, 149.20, 147.25, 137.90, 137.57, 135.07, 131.19, 130.69, 128.93, 127.86, 125.72, 122.53, 104.77, 102.91, 60.86, 56.21, 47.26. Anal. ($C_{25}H_{22}N_2O_5 \cdot 0.6H_2O$) C, H, N.

Compound **1j** was crystallized from chloroform/hexanes as an orange solid: 110 mg (16% yield); mp 215–216 °C dec; TLC (chloroform/methanol [49:1]) $R_f = 0.66$; ^{1}H NMR (500 MHz, $CDCl_3$) δ 8.47 (d, $J = 8.4$ Hz, 1H), 8.12–8.16 (m, 2H), 8.08 (d, $J = 8.4$ Hz, 1H), 7.54–7.48 (m, 3H), 6.54 (s, 2H), 6.36 (t, $J = 5.7$ Hz, 1H), 5.85 (s, 1H), 4.36 (d, $J = 5.7$ Hz, 2H), 3.86 (2s, 9H); ^{13}C NMR (125 MHz, $CDCl_3$) 181.88, 180.20, 160.63, 153.76, 148.04, 146.54, 137.86, 137.57, 135.17, 131.19, 130.36, 129.08, 128.98, 127.54, 124.80, 104.54, 101.33, 60.86, 56.19, 47.25. Anal. ($C_{25}H_{22}N_2O_5 \cdot 0.3H_2O$) C, H, N.

2-(3,4,5-Trimethoxyphyenyl)-6-methoxy-5,8-quinolinedione (1k). Compound **1k** was prepared by the two-step synthesis described below.

To 100 mg (0.310 mmoles) of quinolinedione **4c** in 10 mL of ethanol at room temperature was added 0.34 mmols of piperidine, and the reaction was stirred at room temperature. After the disappearance of starting material by TLC (ethyl acetate), the resulting red precipitate was filtered and washed with cold ethanol and dried under high vacuum to yield 78 mg (62% yield) of analytically pure 2-(3,4,5-trimethoxyphyenyl)-6-piperidino-5,8-quinolinedione: mp, dec >170 °C; TLC (ethyl acetate) $R_f = 0.39$; FTIR (KBr pellet): 804, 1004, 1122, 1236, 1342, 1452, 1566, 1672, 2839, 2937, 3454, cm^{-1}; ^{1}H NMR ($CDCl_3$) δ 8.23 (1H, d), 8.19 (1H, d), 6.01 (1H, s), 3.79 (6H, s), 3.63 (3H, s), 3.40 (3H, m), 3.2 (3H, s), 1.57 (4H, s).

A mixture containing 50 mg (0.123 mmols) of 2-(3,4,5-trimethoxyphyenyl)-6-piperidino-5,8-quinolinedione, 2 mL of methanol, and 92 μL of sulfuric acid were refluxed for two hours. The reaction was cooled and concentrated in vacuo. The resulting residue was neutralized with saturated sodium bicarbonate solution and extracted with ethyl acetate. The organic extracts were dried with sodium sulfate and concentrated. The resulting pale orange solid was recrystallized with ethyl acetate and hexanes to afford 30 mg of pale orange crystals (70% yield): mp, dec >235 °C; TLC (ethyl acetate) $R_f = 0.40$; FTIR (KBr pellet): 808, 1124, 1242, 1342, 1464, 1581, 1678, 2841, 2941, 2993, 3065 cm^{-1}; ^{1}H NMR ($CDCl_3$) δ 8.49 (1H, d, $J = 8.4$), 8.02 (1H, d, $J = 8.4$), 7.41 (2H, s), 6.36 (1H, s), 3.99 (6H, s), 3.95 (3H, s), 3.92 (3H, s); 2D NMR HMBC (see Supporting Information); MS *m/z*. Anal. ($C_{19}H_{17}NO_6 \cdot 0.3H_2O$) C, H, N.

6-Aziridinyl-2-methylquinoline-5,8-dione (2a). To a stirred solution of **4b** (200 mg, 1.16 mmol) in ethanol (15 mL) was added aziridine (184 μL, 3.46 mmol). After 2 h, the resulting precipitate was filtered, washed with ice-cold ethanol, and dried to yield a yellow solid. This was purified by flash chromatography (SiO_2, chloroform/methanol [97:3]) to yield yellow crystals: 54 mg (22% yield); mp 184–185 °C dec; TLC (chloroform/methanol [19:1]) $R_f = 0.63$; ^{1}H NMR (500 MHz, $CDCl_3$) δ 8.30 (d, $J = 8$ Hz, 1H), 7.49 (d, $J = 8$ Hz, 1H), 6.42 (s, 1H), 2.77 (s, 3H), 2.32 (s, 4H); ^{13}C NMR (125 MHz, $CDCl_3$) 183.29, 181.26, 165.12, 157.23, 147.45, 134.63, 126.94, 126.38, 119.76, 27.74, 25.34; MS 214 (M^+), 185, 159, 131, 120, 103, 94. Anal. ($C_{12}H_{10}N_2O_2$) C, H, N.

7-Aziridinyl-3-methoxy-2-methylquinolin-5,8-dione (2b). To a solution of **4e** (250 mg, 1.23 mmol) in ethanol (20 mL) was added aziridine (300 μl, 5.65 mmol) and the mixture was stirred for 2 h. The resulting precipitate was filtered, washed with ice-cold ethanol, and dried to yield an orange solid. This solid was purified by column chromatography (SiO_2, chloroform/ethyl acetate [8:2]) and crystallized from chloroform/hexanes to yield yellow crystals (42 mg, 14%); mp > 210 °C dec; TLC (chloroform/methanol [19:1]) $R_f = 0.73$; ^{1}H NMR (300 MHz, $CDCl_3$) δ 7.62 (s, 1H), 6.26 (s, 1H), 4.00 (s, 3H), 2.63 (s, 3H), 2.32 (s, 4H); ^{13}C NMR (125 MHz, $CDCl_3$) 184.31, 179.14, 158.33, 157.37, 155.03, 139.14, 129.56, 117.85, 111.36, 56.12, 27.83, 20.04; MS 244 (M^+), 229, 217, 202, 189, 146, 104. Anal. ($C_{13}H_{12}N_2O_3$) C, H, N.

7-Aziridinyl-3-methoxy-2-phenylquinolin-5,8-dione (2c). To a stirred solution of **4f** (215 mg, 0.81 mmol) in ethanol (25 mL) was added aziridine (129 μl, 2.43 mmol). After 3 h, the resulting precipitate was filtered, washed with ice-cold ethanol, and dried to yield a yellow solid. This was purified by column chromatography (SiO_2, chloroform/ethyl acetate [8:2]) and crystallized from chloroform/hexanes to yield yellow crystals: 115 mg (46% yield); mp 197 °C dec; TLC (chloroform/methanol [19:1]) $R_f = 0.81$; ^{1}H NMR (500 MHz, $CDCl_3$) δ 8.03 (m, 2H), 7.82 (s, 1H), 7.46 (m, 3H), 6.31 (s, 1H), 4.04 (s, 3H), 2.34 (s, 4H); ^{13}C NMR (125 MHz, $CDCl_3$) 184.02, 178.81, 158.65, 156.92, 152.46, 139.75, 136.04, 129.92, 129.69, 129.63, 128.08, 118.06, 113.93, 56.33, 27.87; MS 306 (M^+), 305, 291, 279, 263, 140. Anal. ($C_{18}H_{14}N_2O_3 \cdot 0.25H_2O$) C, H, N.

6-Aziridinyl-2-(3,4,5-trimethoxyphenyl)quinoline-5,8-dione (2d). To a stirred solution of **4c** (140 mg, 0.43 mmol) in ethanol (20 mL) was added aziridine (200 μL, 3.77 mmol). After 4 h, the resulting precipitate was filtered, washed with ice-cold ethanol, and dried to yield an orange solid. This solid was purified by column chromatography (SiO_2, chloroform/ethyl acetate [7:3]) and crystallized from chloroform/hexanes to yield yellow crystals: 77 mg (49% yield); mp 187–8 °C; TLC (chloroform/methanol [19:1]) $R_f = 0.73$; ^{1}H NMR (500 MHz, $CDCl_3$) 8.44 (d, $J = 8$ Hz, 1H), 7.99 (d, $J = 8$ Hz, 1H), 7.40 (s, 2H), 6.46 (s, 1H), 3.99 (s, 6H), 3.92 (s, 3H), 2.35 (s, 4H); ^{13}C NMR (125 MHz, $CDCl_3$) 182.91, 181.10, 161.64, 157.35, 153.65, 147.77, 140.69, 135.26, 133.05, 126.73, 123.09, 120.03, 105.21, 60.99, 56.39, 27.78; MS 366 (M^+), 351, 323, 293, 265, 209. Anal. ($C_{20}H_{13}N_2O_5 \cdot 0.1H_2O$) C, H, N.

6-Aziridinyl-2-(4-biphenyl)quinoline-5,8-dione (2e). To a stirred solution of **4d** (275 mg, 0.88 mmol) in ethanol (30 mL) was added aziridine (141 μL, 2.65 mmol). After 4 h, the resulting precipitate was filtered, washed with ice-cold ethanol, and dried to yield an orange solid. This solid was purified by column chromatography (SiO_2, chloroform/ethyl acetate [8:2]) and crystallized from chloroform/hexanes to give orange crystals: 157 mg (51% yield); mp 205–7 °C; TLC (ethyl acetate/hexanes [1:1]) $R_f = 0.20$; ^{1}H NMR (400 MHz, $CDCl_3$) δ 8.47 (d, $J = 8$ Hz, 1H), 8.28 (d, $J = 8.4$ Hz, 2H), 8.09 (d, $J = 8$ Hz, 1H), 7.75 (d, $J = 8.4$ Hz, 2H), 7.67 (d, $J = 7.6$ Hz, 2H), 7.48 (t, $J = 7.6$ Hz, 2H), 7.39 (t, $J = 7.6$ Hz, 1H),

6.48 (s, 1H), 2.35 (s, 4H); ^{13}C NMR (100 MHz, $CDCl_3$) δ 183.05, 181.14, 161.56, 157.37, 147.97, 143.46, 140.14, 136.25, 135.34, 128.90, 128.26, 127.90, 127.64, 127.16, 126.90, 123.09, 120.12, 27.78; MS (M^+). Anal. ($C_{23}H_{16}N_2O_2 \cdot 0.2H_2O$) C, H, N. Anal. Calcd ($C_{23}H_{16}N_2O_2.0.2H_2O$): C, 77.60; H, 4.64; N, 7.87. Found: C, 77.37; H, 4.52; N, 7.81.

6-Aziridinyl-3-methyl-2-phenylquinolin-5,8-dione (2f). To a stirred solution of **4g** (300 mg, 1.20 mmol) in ethanol (25 mL) was added aziridine (190 μL, 3.6 mmol). After 1 h, the reaction mixture was filtered, and the precipitate was washed with ice-cold ethanol and dried to yield a yellow solid. The solid was purified by flash chromatography (SiO_2, chloroform/ethyl acetate [8:2]) and crystallized from chloroform/hexanes to give yellow crystals: 170 mg (49% yield); mp 193 °C dec; TLC (chloroform/methanol [19:1]) $R_f = 0.78$; ^{1}H NMR (400 MHz, $CDCl_3$) δ 8.28 (s, 1H), 7.58 (m, 2H), 7.46 (m, 3H), 6.44 (s, 1H), 2.52 (s, 3H), 2.33 (s, 3H); ^{13}C NMR (100 MHz, $CDCl_3$) δ 183.02, 181.56, 164.04, 157.21, 145.58, 138.98, 136.35, 135.74, 129.23, 129.02, 128.31, 126.88, 120.22, 27.76, 20.61; MS 290 (M^+), 262, 248, 234, 220, 205, 191, 166, 139, 115. Anal. ($C_{18}H_{14}N_2O_2$) C, H, N.

Antiangiogenesis Assays. Growth inhibition and cord formation assays were conducted using human umbilical vein endothelial cells (HUVEC) purchased from BD Biosciences. HUVEC cells were grown in EGM-2 medium (Cambrex).

Growth Inhibition Assay. The standard sulforhodamine B assay was used to assess growth inhibition. Briefly, cells were inoculated in 96-well plates and incubated for 24 h. Serial dilutions of the compounds were then added. After 48 h, the plates were fixed with trichloroacetic acid, stained with sulforhodamine B, and read with an automated plate reader. A growth inhibition of 50% (GI_{50} or the drug concentration causing a 50% reduction in the net protein increase) was calculated from optical density data with Immunosoft software.

Cord Formation Assay. Matrigel, a basement membrane matrix, was purchased from BD Biosciences. An aliquot of 60 μL was placed in each well of an ice-cold 96-well plate. The plates were left 15 min at room temperature and then incubated for 30 min at 37 °C to permit the material to gel. Meanwhile, HUVEC were harvested and diluted to a concentration of 2×10^5 cells/mL. Cell suspension (100 μL) was added to each well. The compounds to be tested were then added in an additional 100 μL of culture medium. After 24 h of incubation, images were acquired using an inverted Nikon Diaphot 300 and DXM1250F Nikon digital camera. Drug effects were assessed and compared with untreated controls by measuring the length of cords formed and the number of junctions.

Acknowledgment. We thank the Arizona Disease Control Research Commission for their generous support.

Supporting Information Available: Elemental analyses, 2D NMR HMBC of **1k**, and detailed antiangiogenesis assay results are included. This material is available free of charge via the Internet at http://pubs.acs.org.

References

(1) Vinogradov, S.; Roig, V.; Sergueeva, Z.; Nguyen, C. H.; Arimondo, P.; Thuong, N. T.; Bisagni, E.; Sun, J. S.; Helene, C.; Asseline, U. Synthesis and binding properties of oligo-2′-deoxyribonucleotides conjugated with triple-helix-specific intercalators: Benzo[e] and benzo(G] pyridoindoles. *Bioconjugate Chem.* **2003**, *14*, 120–135.

(2) Neckers, L. Hsp90 inhibitors as novel cancer chemotherapeutic agents. *Trends Mol. Med.* **2002**, *8*, S55–S61.

(3) Neckers, L.; Schulte, T. W.; Mimnaugh, E. Geldanamycin as a potential anti-cancer agent: Its molecular target and biochemical activity. *Invest. New Drugs* **1999**, *17*, 361–373.

(4) Andrus, M. B.; Meredith, E. L.; Simmons, B. L.; Sekhar, B. B. V. S.; Hicken, E. J. Total synthesis of (+)-geldanamycin and (−)-*o*-quinogeldanamycin with use of asymmetric anti- and syn-glycolate aldol reactions. *Org. Lett.* **2002**, *4*, 3549–3552.

(5) Andrus, M. B.; Meredith, E. L.; Sekhar, B. B. V. S. Synthesis of the left-hand portion of geldanamycin using an antiglycolate aldol reaction. *Org. Lett.* **2001**, *3*, 259–262.

(6) Nimmanapalli, R.; OBryan, E.; Bhalla, K. Geldanamycin and its analogue 17-allylamino-17-demethoxygeldanamycin lowers Bcr-Abl levels and induces apoptosis and differentiation of Bcr-Abl-positive human leukemic blasts. *Cancer Res.* **2001**, *61*, 1799–1804.

(7) Chiosis, G.; Lucas, B.; Shtil, A.; Huezo, H.; Rosen, N. Development of a purine-scaffold novel class of Hsp90 binders that inhibit the proliferation of cancer cells and induce the degradation of Her2 tyrosine kinase. *Bioorg. Med. Chem.* **2002**, *10*, 3555–3564.

(8) Chiosis, G.; Timaul, M. N.; Lucas, B.; Munster, P. N.; Zheng, F. F.; Sepp-Lorenzino, L.; Rosen, N. A small molecule designed to bind to the adenine nucleotide pocket of Hsp90 causes Her2 degradation and the growth arrest and differentiation of breast cancer cells. *Chem. Biol.* **2001**, *8*, 289–299.

(9) Lucas, B; Rosen, N; Chiosis, G. Facile synthesis of a library of 9-alkyl-8-benzyl-9*H*-purin-6-ylamine derivatives. *J. Comb. Chem.* **2001**, *3*, 518–20.

(10) Hargreaves, R.; David, C. L.; Whitesell, L.; Skibo, E. B. Design of quinolinedione-based geldanamycin analogues. *Bioorg. Med. Chem. Lett.* **2003**, *13*, 3075–3078.

(11) Paull, D. K.; Shoemaker, R. H.; Hodes, L.; Monks, A.; Scudiero, D. A.; Rubinstein, L.; Plowman, J.; Boyd, M. R. Display and analysis of differential activity of drugs against human tumor cell lines: Development of mean graph and COMPARE algorithm. *J. Natl. Cancer Inst.* **1989**, *81*, 1088–1092.

(12) Sausville, E. A.; Zaharevitz, D.; Gussio, R.; Meijer, L.; Louarn-Leost, M.; Kunick, C.; Schultz, R.; Lahusen, T.; Headlee, D.; Stinson, S.; Arbuck, S. G.; Senderowicz, A. Cyclin-dependent kinases: Initial approaches to exploit a novel therapeutic target. *Pharmacol. Ther.* **1999**, *82*, 285–292.

(13) Showalter, H. D. H.; Pohlmann, G. An improved synthesis of 4,7-dimethoxy-1*H*-indole. *Org. Prep. Proced. Int. Briefs* **1992**, *24*, 484–488.

(14) Marcu, M. G.; Schulte, T. W.; Neckers, L. J. Novobiocin and related coumarins and depletion of heat shock protein 90-dependent signaling proteins. *J. Natl. Cancer Inst.* **2000**, *92*, 242–248.

(15) Whitesell, L.; Mimnaugh, E. G.; DeCosta, B.; Myers, C. E.; Neckers, L. M. Inhibition of heat shock protein HSP90-pp60v-src heteroprotein complex formation by benzoquinone ansamycins: Essential role for stress proteins in oncogenic transformation. *Proc. Natl. Acad. Sci. U.S.A.* **1994**, *91*, 8324–8328.

(16) Bagatell, R.; Paine-Murrieta, G. D.; Taylor, C. W.; Pulcini, E. J.; Akinaga, S.; Benjamin, I. J.; Whitesell, L. Induction of a heat shock factor 1-dependent stress response alters the cytotoxic activity of Hsp90-binding agents. *Clin. Cancer Res.* **2000**, *6*, 3312–3318.

(17) Boyd, M. R. *Principles and Practices of Oncology (PPO updates)*; J.B. Lippincott: Phildelphia, PA, 1989; pp 1–12.

(18) Lanza, D. L.; Yost, G. S. Selective dehydrogenation/oxygenation of 3-methylindole by cytochrome P450 enzymes. *Drug Metab. Dispos.* **2001**, *29*, 950–953.

(19) Bassett, S.; Urrabaz, R.; Sun, D. Cellular response and molecular mechanism of antitumor activity by leinamycin in MiaPaCa human pancreatic cancer cells. *Anti-Cancer Drugs* **2004**, *15*, 689–696.

(20) Thompson, J. E.; Thompson, C. B. Putting the rap on akt. *J. Clin. Oncol.* **2004**, *22*, 4217–4226.

(21) Xing, C.; Skibo, E. B.; Dorr, R. T. Aziridinyl quinone antitumor agents based on indoles and cyclopent[*b*]indoles: Structure−activity relationships for cytotoxicity and antitumor activity. *J. Med. Chem.* **2001**, *44*, 3545–3562.

(22) Ross, D. T.; Scherf, U.; Eisen, M. B.; Perou, C. M.; Rees, C.; Spellman, P.; Iyer, V.; Jeffrey, S. S.; Van De Rijn, M.; Waltham, M.; Pergamenschikov, A.; Lee, J. C. E.; Lashkari, D.; Shalon, D.; Myers, T. G.; Weinstein, J. N.; Botstein, D.; Brown, P. O. Systematic variation in gene expression patterns in human cancer cell lines. *Nat. Genet.* **2000**, *24*, 227–235.

(23) Itokawa, H.; Matsumoto, K.; Morita, H.; Takeya, K. Cytotoxic naphthoquinones from *Mansoa alliacea*. *Phytochemistry* **1992**, *31*, 1061–2.

(24) Turowski, P.; Franckhauser, C.; Morris, M. C.; Vaglio, P.; Fernandez, A.; Lamb, N. J. Functional cdc25C dual-specificity phosphatase is required for S-phase entry in human cells. *Mol. Biol. Cell* **2003**, *14*, 2984–2998.

(25) Murphy, P. V.; Pitt, N.; O'Brien, A.; Enright, P. M.; Dunne, A.; Wilson, S. J.; Duane, R. M.; O'Boyle, K. M. Identification of novel inhibitors of fibroblast growth factor (FGF-2) binding to heparin and endothelial cell survival from a structurally diverse carbohybrid library. *Bioorg. Med. Chem. Lett.* **2002**, *12*, 3287–3290.

(26) Aviezer, D.; Seddon, A. P.; Wildey, M. J.; Bohlen, P.; Yayon, A. Development of a high-throughput screening assay for inhibitors of fibroblast growth factor-receptor-heparin interactions. *J. Biomol. Screen.* **2001**, *6*, 171–177.

(27) Manetti, F.; Corelli, F.; Botta, M. Fibroblast growth factors and their inhibitors. *Curr. Pharm. Des.* **2000**, *6*, 1897–1924.

(28) Nam, N. H. Combretastatin A-4 analogues as antimitotic antitumor agents. *Curr. Med. Chem.* **2003**, *10*, 1697–1722.
(29) Loneragan, G. H.; Gould, D. H.; Mason, G. L.; Garry, F. B.; Yost, G. S.; Lanza, D. L.; Miles, D. G.; Hoffman, B. W.; Mills, L. J. Association of 3-methyleneindolenine, a toxic metabolite of 3-methylindole, with acute interstitial pneumonia in feedlot cattle. *Am. J. Vet. Res.* **2001**, *62*, 1525–1530.
(30) Ghodousi, A.; Huang, X.; Cheng, Z.; Skibo, E. B. Pyrrolobenzimidazoles (PBIs) linked to heterocycles and peptides. Design of DNA base pair specific phosphate hydrolyzing agents and novel cytotoxic agents. *J. Med. Chem.* **2004**, *47*, 90100.

JM7014099